Orthotropic Viscoelastic Properties of Chinese Fir Wood Saturated with Water in Frozen and Non-frozen States

Zhu Li
Jiali Jiang
Jianxiong Lyu
Jinzhen Cao

Abstract

In order to better understand the differences in orthotropic viscoelastic properties of Chinese fir (*Cunninghamia lanceolata*) in frozen and non-frozen states, the storage modulus (E') and loss modulus (E'') of the longitudinal, radial, and tangential specimens were investigated under water-saturated conditions with temperatures ranging from −120°C (or 30°C) to 280°C. Results revealed that the order of magnitude in E' for each orientation was consistent for temperatures below 0°C, while the anisotropy in E' was reduced due to the enhancement effect of ice. Frequency-dependent γ-relaxation was observed at approximately −96°C for all orthotropic directions. A sharp discontinuity in E' occurred at approximately 0°C for each specimen, together with the corresponding sharp peak in the E'' spectrum. Furthermore, the frozen free water had an effect on the orthotropic viscoelastic behavior in the water-saturated specimens within the range of −120°C to 280°C. Specimens with a frozen history leveled off at the initial temperature ramping phase for each orientation, while a frozen history reduced the decline in stiffness of the wood specimens. Similar to the variations in E', the dramatic loss of water increased the complexity of the E'' values. The loss of free water also had a pronounced effect on the viscoelastic properties during the temperature ramping process. Thus, in the wood industry, it necessary to consider the variations in the orthotropic viscoelastic performance of specimens under water-saturated conditions during the water loss process.

In cold climate zones, when fresh-cut logs or timber are stored in an open yard at negative temperatures, the free water inside the wood freezes. The fresh-cut logs or timber are subsequently used for furniture, interior decoration, or building materials, making wood drying an essential process for the wood industry (Han et al. 2017; Baranski 2018; Zhou et al. 2020). Therefore, understanding the impact of frozen free water in the cell lumens and other void spaces on the wood drying properties is crucial. In the current study, we present the viscoelastic properties of the frozen and non-frozen wood in order to determine the impact of the frozen state on the viscoelastic properties of wood during the drying process.

Numerous studies have investigated the physical and mechanical phenomena occurring following the freezing of free water inside wood (Sellevold et al. 1975; Hirsh et al. 1989; Furuta et al. 2001; Li et al. 2020a). Sellevold et al. (1975) observed relaxation at approximately –95°C in specimens at the fiber saturation point (FSP) or with free water. The study also determined the formation of ice to have a slight influence on the loss factor peak, playing a limited role in the adsorbate transition for large differences in the moisture content (MC). Furthermore, Furuta et al. (2001) measured the thermal-softening properties of polysaccharide solutions and identified the possible cause of a relaxation at approximately −120°C of water molecules in a

The authors are, respectively, Doctoral Candidate, Research Inst. of Wood Industry of Chinese Academy of Forestry, Hunan Collaborative Innovation Center for Effective Utilizing of Wood & Bamboo Resources, Beijing, China and College of Materials Sci. and Technol., Beijing Forestry Univ., Beijing, China (lizhu@caf.ac.ac.cn); Professor, Research Inst. of Wood Industry of Chinese Academy of Forestry, Hunan Collaborative Innovation Center for Effective Utilizing of Wood & Bamboo Resources, Beijing, China (jialiwood@caf.ac.cn, jianxiong@caf.ac.cn [corresponding author]); and Professor, College of Materials Sci. and Technol., Beijing Forestry Univ., Beijing, China (caoj@bjfu.edu.cn [corresponding author]). This paper was received for publication in October 2020. Article no. 20-00069.

Forest Prod. J. 71(1):77–83.
doi:10.13073/FPJ-D-20-00069

high polymeric gel. In our previous research, the freezing of free water in the wood cell lumens resulted in the modification of the relaxation mechanism in wood below −108°C. This may be related to the amorphous wood cell wall coupling to ice during the quenching process (Li et al. 2020a). Based on the observations of specimens with free water at ultralow temperatures, exploring the impact of frozen free water on the viscoelastic properties of wood at temperatures below 0°C is of particular interest.

Temperature has a strong influence on the viscoelastic behavior of wood polymers. Variations in temperature can alter the internal binding energy and further influence the average distance between molecules (Zhao et al. 2016). In addition, the moisture in wood and its variation rate are strongly associated with temperature. Thus, the dual effects of temperature and MC on the viscoelastic properties of wood are considerably complex (Engelund and Salmén 2012; Zhan et al. 2016; Li et al. 2020b). The release of the water molecules outside of the wood cell walls unbalances the specimen conditions, altering the viscoelastic behavior and resulting in stresses and shrinkages. Variations in MC can lead to an unstable state within the wood cell walls (Habeger and Coffin 2000; Takahashi et al. 2004; Zhan et al. 2016). Under an external load, the unstable state enhances the flexibility of the polymer network and triggers the mechano-sorptive effect (Zhan et al. 2019; Peng et al. 2020). This phenomena is prominent in the water-saturated specimens (Zhan et al. 2015). Furthermore, at temperatures above 180°C, the cleavage of chemical bonds and the degradation and rearrangement of wood components can occur in the wood cell walls (Alén et al. 2002; Guo et al. 2015; Li et al. 2020b). This consequently increases the complexity of the temperature dependence of the wood viscoelastic properties. Therefore, more information on the relationship between the viscoelasticity and temperature of the water-saturated specimens is required.

Dynamic mechanical analysis (DMA) is an effective method for the study of the viscoelastic properties of wood polymers. DMA is able to separately define the elastic and damping properties of wood polymers, thus providing insights into the organization and properties of in situ wood polymers over a wide temperature range (Sun et al. 2007; Chowdhury et al. 2010). In the present study, the orthotropic viscoelastic properties of Chinese fir (*Cunninghamia lanceolata*) under water-saturated conditions in frozen and non-frozen states were investigated over a wide temperature range from −120°C to 280°C, with the aim of further understanding the viscoelastic behavior in wood polymers with a history of free water frozen.

Materials and Methods

Wood materials

Clear wood specimens in the longitudinal (L), radial (R), and tangential (T) grain orientations from Chinese fir heartwood were cut into dimensions of 35 mm by 6 mm by 1.5 mm (length, width, thickness) between the 6th and 14th growth rings (Fig. 1). Before testing, all specimens were stored in distilled water at room temperature for more than 3 months until the water-swollen state was reached. The specimens did not float in distilled water following this treatment. Table 1 reports the average basic density and MC prior to the measurements.

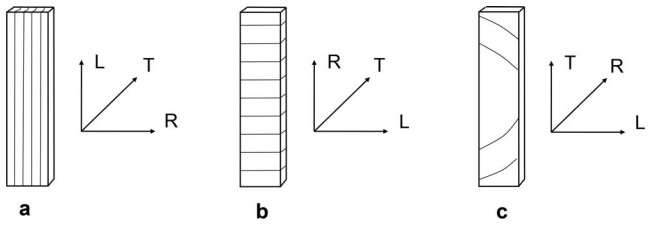

Figure 1.—Schematic of Chinese fir wood specimens for all orthotropic directions. (a) longitudinal (L); (b) radial (R); and (c) tangential (T).

Experimental methods

The viscoelastic properties of the specimens were measured via a dynamic mechanical analyzer (DMA 2980, TA Instruments) with a cooling accessory. The cooling system uses cold nitrogen gas generated from the controlled evaporation of liquid nitrogen. In order to minimize the influence of moisture variation, specimens were tested immediately following the removal from the distilled water. A tensile mode with 18 mm between clamping midpoints was selected. Specimens were secured with a clamping torque of 0.7 N.m. The preload force, displacement amplitude, and force track were set as 0.01 N, 15 μm and 125 percent, respectively, with measurement frequencies of 0.5, 1, 2, 5, and 10 Hz.

The testing of the measured temperature included two procedures. In procedure A, the temperature decreased rapidly from room temperature to −120°C and was subsequently maintained constant at −120°C for 10 minutes. A temperature scan from −120°C to 280°C was then conducted with a programmed heating rate of 2°C/min. During procedure B: the temperature scan was performed directly between 30°C and 280°C for the same heating rate of 2°C/min. For each condition, three replicates were tested, with a single representative curve for each replicate shown in the following figures. The results of the dynamic mechanical analysis are commonly presented as: (1) the storage modulus (E'), describing the capacity of the material to support a load and represents the elastic components of the material; and (2) the loss modulus (E''), namely, the viscous response of the material and is proportional to its dissipated energy.

Results and Discussion

Average wood density and MC

Table 1 reports the average basic density and MC of the water-saturated specimens in all orthotropic directions. The average MC values of the water-saturated specimens in the L, R, and T grain orientations were determined as 302.7, 309.1, and 296.9 percent, with coefficients of

Table 1.—Basic density and moisture content (MC) of water-saturated wood specimens in the L, R, and T grain orientations. Coefficient of variation values obtained after the repetition of the measurements are also given.

Physical properties	L	R	T
Basic density (kg/m^3)	269.8 ± 5.7%	256.9 ± 2.8%	259.6 ± 1.8%
MC (%)	302.7 ± 3.3%	309.1 ± 3.1%	296.9 ± 2.5%

variation of 3.3, 3.1, and 2.5 percent, respectively. Specimens in the R direction demonstrated a higher MC value than those in the L and T directions. In general, the difference in MC among different structural directions was influenced by its specific structure. Chinese fir wood primarily consists of tracheids, which are aligned in the L direction. In addition, MC is associated with the bulk density of wood, where the lower basic density of the R specimens provides a greater amount of specific surface area and void spaces. Consequently, the R specimens absorbed more moisture than the L and T specimens during the process of water uptake.

Orthotropic viscoelasticity of temperatures between −120°C and 280°C

Figure 2 presents the temperature dependence of the tensile storage modulus (E') and loss modulus (E'') for the L, R, and T specimens under water-saturated conditions and at a frequency of 10 Hz. At the initial measured temperature of −120°C, the E' values of the specimens were determined as 6573 MPa, 4667 MPa, and 4333 MPa in the L, R, and T directions, respectively. This order of magnitude was consistent for each orientation. Compared with those in the non-frozen state, an enhancement of E' by up to one to two orders of magnitude was observed for the water-saturated specimens in the transverse directions at temperatures below 0°C. This implies the ability of the frozen free water in the wood cell lumens to increase E' values, agreeing with previous studies (Sellevold et al. 1975; Furuta et al. 2001; Gao et al. 2015; Li et al. 2020a). The same trend was observed for E'' values in the R and T directions. At temperatures below 0°C, the modulus was relatively high and the material apparently stable. The E'' of specimens in transverse directions below 0°C was large and five to ten times higher than those in the non-frozen state. This suggests that the E'' values in the transverse directions did not change significantly for temperatures above 0°C (Fig. 2). Thus, it can be concluded that the values of anisotropy in the viscoelastic parameters at −120°C were lower than those of the corresponding values at temperatures above 0°C, which demonstrates the reduction in the anisotropy of Chinese fir wood due to the enhancement effect of ice. The crystalline cellulose microfibrils, which play an important role in the properties of the L specimens, were orientated in the L direction during the tensile tests (Li et al. 2018; Peng et al. 2020). Therefore, the modulus of the L specimens was not observed to enhance by a large margin, despite the formation of ice in the wood cells.

Interestingly, a sharp discontinuity in E' occurred close to 0°C for each specimen irrespective of grain orientation, together with the corresponding sharp peak within the E'' temperature spectrum. The dramatic shift in the modulus close to the freezing point is evident and is attributed to the phase transformation of free water in the wood cell cavities. This is consistent with previous studies (Sellevold et al. 1975; Furuta et al. 2001; Gao et al. 2015). The peak temperatures of the specimens exhibited a clear grain orientation at approximately 10°C, 5°C, and 6°C in the L, R, and T directions, respectively. The peak temperatures in the L specimens were evidently higher than those in the transverse directions. Supplementary Figure S1 presents the viscoelastic parameter values at each orientation for additional frequencies. The E'' peak location close to 0°C was approximately constant, thus demonstrating an independence of the measurement frequency, and may consequently be linked to the melting of ice (Furuta et al. 2001). However, the E'' peak intensities exhibited a marked decrease with increasing measured frequency for all orthotropic directions.

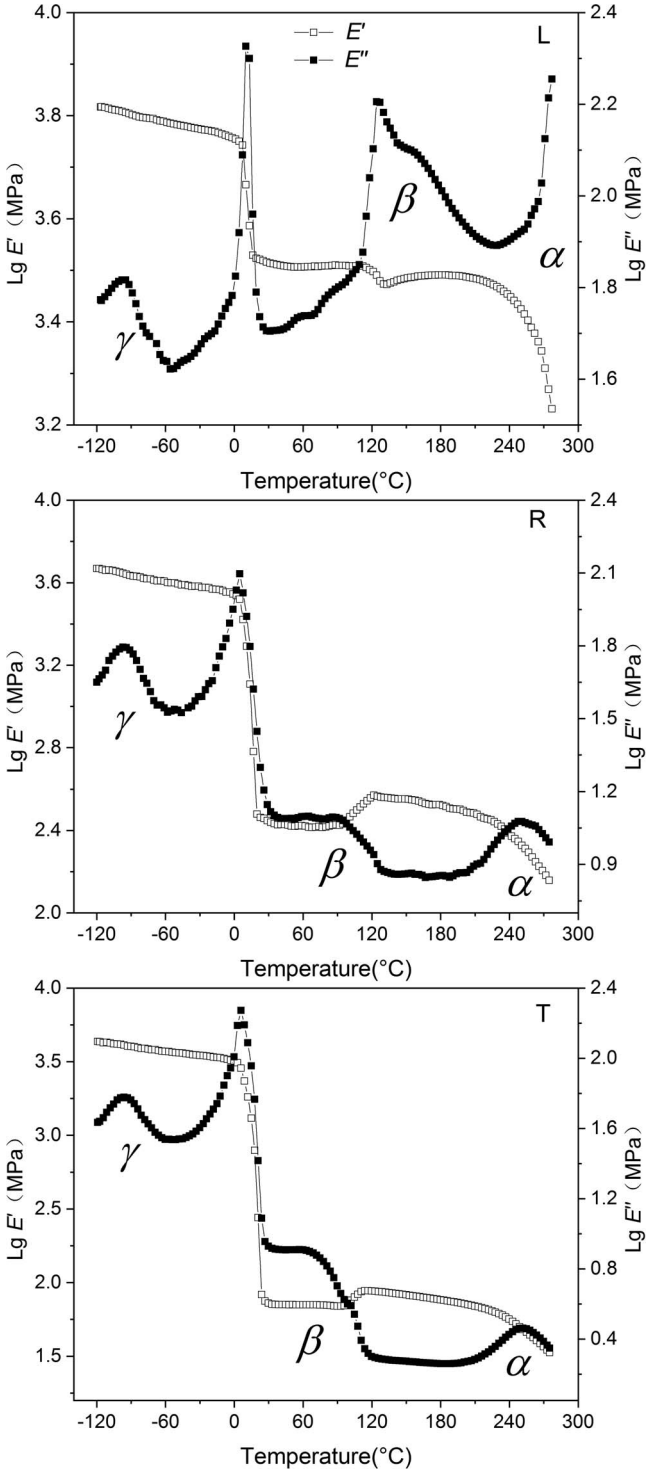

Figure 2.—Temperature dependence of the tensile storage modulus (E′) and loss modulus (E″) for the L, R, and T specimens under water-saturated condition at a frequency of 10 Hz.

A clear relaxation process for E'' about –96°C was observed in all wood specimens, denoted as the γ-relaxation (Fig. 2). More specifically, the peak temperature of the γ-relaxation and the corresponding E'' values were –95°C, –97°C, and –96°C; 66 MPa, 62 MPa, and 60 MPa in the L, R, and T specimens, respectively. Minimal differences were determined in the peak temperatures and intensities of the γ-relaxation. This result may be related to the varying free water content and specific wood structure in the three anatomic directions. The γ-relaxation did not exhibit any obvious grain orientation. Furthermore, the peak temperature location of the γ-relaxation depended on the measurement frequency, while the E'' peak temperature shifted to a lower temperature range for a decreasing measured frequency (Supplementary Fig. S1). Similar observations have been reported for polysaccharide solutions (Furuta et al. 2001). The molecular motion of the wood polymers was generally influenced by frequency and temperature. The γ-relaxation was not observed at relative lower frequencies (0.5 Hz). Smaller scale molecular movements in the wood cells were observed at relatively higher measured frequencies (Zhan et al. 2019). Sellevold et al. (1975) observed γ-relaxation peak temperatures in the loss factor (tan δ) temperature spectrum for the L specimens with MCs of 26, 96, and 98 percent at –97°C, –95°C, and –96°C, respectively. The authors attributed the transition to the gradual solidification of the adsorbed water. In the current study, a similar transition at –95°C was observed for L specimens under water-saturated conditions. However, our previous research demonstrated a clear grain orientation for the γ-relaxation within a similar temperature range (Li et al. 2018), with γ-relaxation peak temperatures of –101°C, –85°C, and –81°C in the L, R, and T specimens at a frequency of 10 Hz, respectively. Therefore, we attribute the change in the γ-relaxation mechanism observed in the current study to the freezing of the free water in the wood cell lumens. The molecular mobility at low temperatures is influenced by the surrounding environment (Roig et al. 2017). We observed a dependance of the γ-relaxation on the measurement frequency, yet no evident grain orientation was identified. Therefore, we assign the γ-relaxation at around –96°C to the frozen free water molecules in the wood cell lumens.

Figure 3 depicts the temperature dependence of E' and E'' for specimens at the FSP condition for each orientation at a frequency of 10 Hz. The desired 100 percent relative humidity was maintained via distilled water in climatic chambers, and the corresponding equilibrium moisture content of specimens was taken as the FSP (Li et al. 2018). Data of the orthotropic viscoelastic properties in Figure 3 are taken from our previous study based on the same method (Li et al. 2018, 2020b). The results clearly indicate the dependance of E' and E'' on grain orientation. With respect to E'', the three relaxation processes were observed for all specimens, irrespective of grain orientations, throughout the –120°C to 280°C temperature range. In addition, for temperatures between 40°C and 100°C, the E' did not decrease monotonically with increasing temperature due to the loss of moisture. The variation in the viscoelastic parameters for all wood specimens above 30°C will be discussed in detail below. The formation of ice in the wood cell lumens not only had an effect on the orthotropic viscoelastic properties in specimens at temperatures below 0°C, but also altered the manifestation of the relaxation process above 0°C. In general, no fundamental changes in the physical and mechanical properties of the free water specimens were detected as a function of MC above 0°C. However, the damping of water-saturated specimens with a frozen history varied with the MC. We thus conclude the orthotropic viscoelastic properties in the water-saturated specimens to be distinct from specimens containing just adsorbed water in the wood cell walls, even at the FSP.

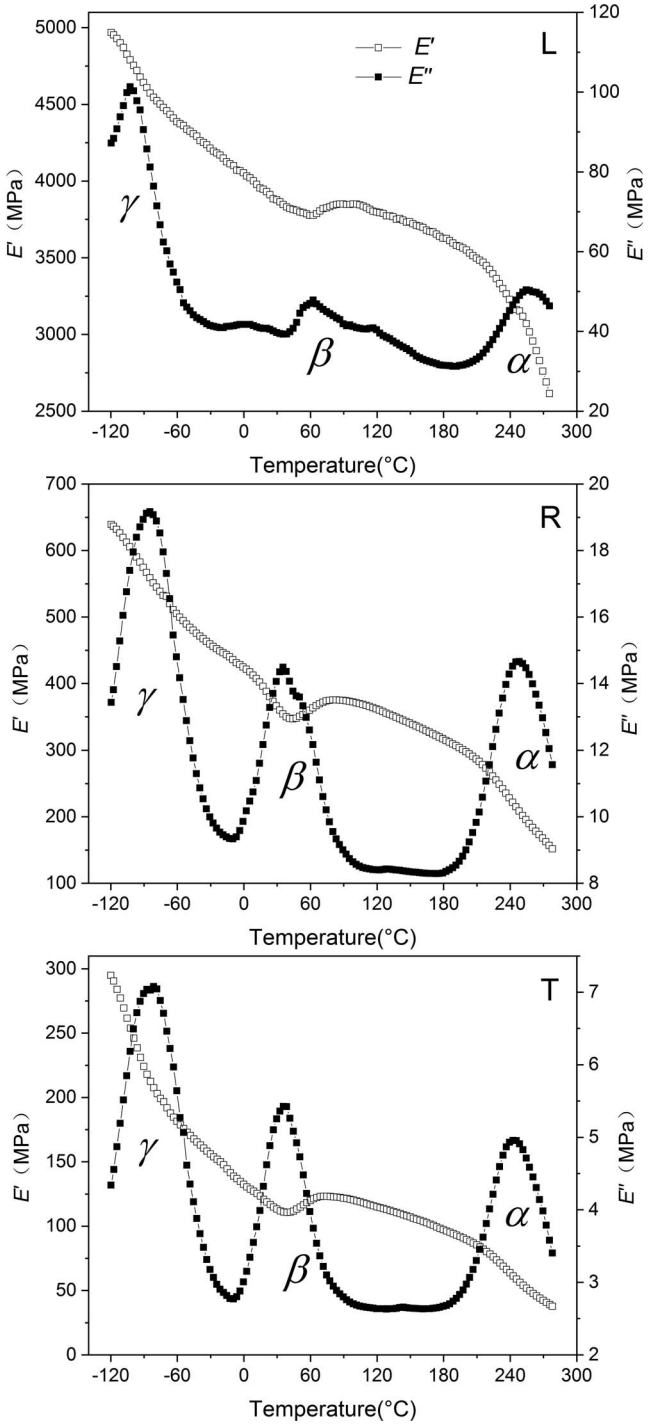

Figure 3.—Temperature dependence of the tensile storage modulus (E′) and loss modulus (E″) for the L, R, and T specimens at the fiber saturation point at a frequency of 10 Hz.

Effect of frozen history on orthotropic viscoelasticity

Figure 4 presents the temperature dependence of the normalized E' (nE', open symbols) and normalized E'' (nE'', filled symbols) at a frequency of 10 Hz between 30°C and 280°C. The normalized viscoelastic parameters were calculated as follows:

$$nE'_{(T)} = E'_{(T)}/E'_{(30)} \quad (1)$$

$$nE''_{(T)} = E''_{(T)}/E''_{(30)} \quad (2)$$

where the subscript ''30'' denotes the corresponding data at 30°C.

Considerable variations were observed for both nE' and nE'' between the water-saturated specimens and those only containing adsorbed water in the wood cell walls. This result may be attributed to the frozen history, as well as the loss of free water within the wood cell lumens. For specimens with the temperature scan from 30°C to 280°C directly, the nE' values initially exhibited a decline, followed by a slight increase and subsequent decrease, regardless of grain orientation. The nE' was initially stable at the temperature ramping phase for all specimens with a frozen history. These results revealed that the hardening of the wood cell wall polymers and the increasing bonding strength of the hydrogen groups in the molecular chain of the wood polymers at low temperatures (Gerhards 1982; Ayrilmis et al. 2010; Zhao et al. 2015) still played a role during the heating process, which compensated for the decline in wood stiffness due to the heating energy. Compared with specimens in the non-frozen state, those with a frozen history exhibited higher nE' values at each temperature, with the exception of the R specimens at 90°C to 120°C, which indicated the suppression of the reduction in wood stiffness due to the frozen history.

Since the experiments were performed in a non–climate-controlled chamber, the water-saturated specimens began to lose free water at relative lower temperatures (i.e., at 30°C) (Zhan et al. 2015). As expected, the wood cell walls shrunk for MC values lower than the FSP. As the temperature increased, the adsorbed water detached from the wood cell walls, resulting in a loss of moisture and an increase in wood stiffness (Zhan et al. 2015; Li et al. 2020b). The nE' values were observed to increase by 4.5, 45.3, and 36.1 percent for specimens with a frozen history in the L, R, and T directions; and 8.1, 43.4, and 25.1 percent with the direct heating process, respectively (Fig. 4). Moreover, specimens at the FSP exhibited increments in nE' of 2.0, 8.2, and 11.3 percent, respectively (Fig. 3). The nE' values experienced a greater increase for water-saturated specimens compared with those at the FSP, irrespective of grain orientations. This confirms the effect of the loss of free water on the specimen stiffness during the heating process. Furthermore, the increment in nE' for the L direction was lower than that of the transverse directions. This indicates that the increasing nE' was more sensitive to moisture changes in the transverse directions compared with the L direction. The inhomogeneity in the wood stiffness of the specimens with the three grain orientations may result in the cracking of wood during the drying process.

With respect to the nE'', two obvious relaxation processes (β-relaxation and α-relaxation) were observed in all specimens above 30°C (Fig. 4). Along with the results in Figure 3, this highlights the variation in nE'' for the water-saturated specimens, which became more complex for each orientation with the dramatic loss of water. The nE'' values decreased together with the increment in nE', irrespective of

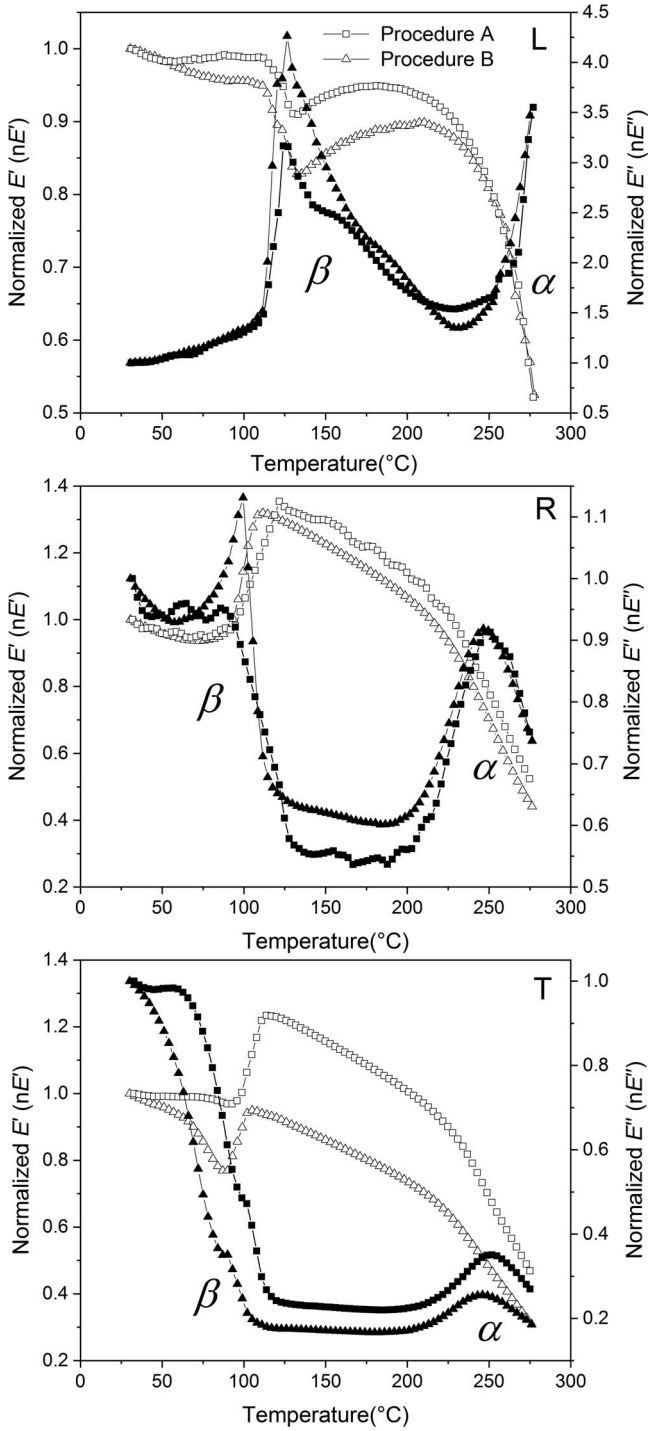

Figure 4.—Effects of the frozen history on the normalized E′ (nE′, open symbols) and normalized E″ (nE″, filled symbols) for the L, R, and T specimens. Procedure A (Squares), the temperature decreased rapidly to −120°C and kept constant for 10 minutes, and then increased from −120°C to 280°C; Procedure B (Triangle), the temperature scan increased from 30°C to 280°C directly.

grain orientations. This result may be a result of the decreased damping and elevated stiffness from the rearrangement of hydrogen bonds (RHB) during moisture desorption (Engelund and Salmén 2012; Zhan et al. 2016, 2018). In addition, the wood cell walls were unstable during the water loss process, while the formation of free volumes (FV) and the temperature-derived segmental motions of wood polymer increased the damping (Takahashi et al. 2004; Zhan et al. 2016). It was therefore speculated that the dominant influence of the RHB is over the multiple effects of the FV and the temperature-derived segmental motions, which behaved as the decrement in the values of nE''. More interestingly, there was a marked reduction in nE'' for T specimens at temperatures ranging from 30°C to 100°C. The decline in nE'' reflects the prevailing effect of the RHB during the water loss process, which is more pronounced in the T direction.

A relaxation process around 250°C α-relaxation was observed in the transverse directions, but not in the L specimens. The α-relaxation was assumed to relate to the micro-Brownian motions of the wood cell wall polymers in the noncrystalline region (Sugiyama et al. 1998; Jiang and Lu 2008). These differences in the longitudinal and transverse directions indicated that the wood mechanical relaxation phenomenon was affected by its orthotropic structure. According to our previous study (Li et al. 2020b), the relaxation peak temperatures close to 250°C in the L specimens were higher than those of the R and T specimens. Therefore, it was speculated that the peak α-relaxation temperatures in the L direction shifted toward higher temperatures over 280°C.

Conclusions

In the current study, the orthotropic viscoelastic behaviors of Chinese fir wood in frozen and non-frozen states were investigated over a wide temperature range from –120°C to 280°C. The storage modulus (E') and loss modulus (E'') parameters were determined in order to improve our understanding of the anisotropic nature of wood under water-saturated conditions.

At each orientation, the values of E' were the same order of magnitude for temperatures below 0°C, while the E' values increased by up to one to two orders of magnitude in the transverse directions. Moreover, a sharp discontinuity was observed for E', together with a corresponding sharp peak in the E'' spectrum. This location of the E'' peak was independent of the measurement frequency, with peak temperatures at around 10°C, 5°C, and 6°C for the L, R, and T specimens, respectively. The γ-relaxation was observed at approximately –96°C for all orthotropic directions and was a function of the measurement frequency, which was assigned to the frozen free water molecules in the wood cell lumens. There was no evidence of grain orientation in the peak temperatures and intensities of the γ-relaxation.

The formation of frozen free water in the wood cell lumens had an effect on the viscoelastic behavior in the water-saturated specimens within the range of –120°C to 280°C. Specimens with a frozen history leveled off at the initial temperature ramping phase for each orientation, while specimens with a frozen history diminished the decrement in wood stiffness. Variations in nE' were influenced by the dual effects of temperature elevation and water loss. The E'' values for each orientation became more complex as E' varied in relation to the dramatic loss of water. Furthermore, the loss of free water also had a pronounced effect on the viscoelastic properties during the heating process. Therefore, it is necessary to consider the difference in the orthotropic viscoelastic performance of specimens under water-saturated conditions during the water loss process.

Acknowledgments

This research was financially supported by the National Natural Science Foundation of China (No. 31971591).

Literature Cited

Alén, R., R. Kotilainen, and A. Zaman. 2002. Thermochemical behavior of Norway spruce (*Picea abies*) at 180–225 °C. *Wood Sci. Technol*. 36(2):163–171.

Ayrilmis, N., U. Buyuksari, and N. As. 2010. Bending strength and modulus of elasticity of wood-based panels at cold and moderate temperatures. *Cold Reg. Sci. Technol*. 63(1–2):40–43.

Baranski, J. 2018. Moisture content during and after high- and normal-temperature drying processes of wood. *Drying Technol*. 36(6):751–761.

Chowdhury, S., J. Fabiyi, and C. E. Frazier. 2010. Advancing the dynamic mechanical analysis of biomass: Comparison of tensile-torsion and compressive-torsion wood DMA. *Holzforschung* 64(6):747–756.

Engelund, E. T. and L. Salmén. 2012. Tensile creep and recovery of Norway spruce influenced by temperature and moisture. *Holzforschung* 66(8):959–965.

Furuta, Y., Y. Obata, and K. Kanayama. 2001. Thermal-softening properties of water-swollen wood: The relaxation process due to water soluble polysaccharides. *J. Mater. Sci*. 36:887–890.

Gao, S., X. M. Wang, and L. H. Wang. 2015. Modeling temperature effect on dynamic modulus of elasticity of red pine (*Pinus resinosa*) in frozen and non-frozen states. *Holzforschung* 69(2):233–240.

Gerhards, C. C. 1982. Effect of moisture content and temperature on the mechanical properties of wood: An analysis of immediate effects. *Wood Fiber* 14:4–36.

Guo, J., K. L. Song, L. Salmén, and Y. F. Yin. 2015. Changes of wood cell walls in response to hygro-mechanical steam treatment. *Carbohyd. Polym*. 115:207–214.

Habeger, C. C. and D. W. Coffin. 2000. The role of stress concentrations in accelerated creep and sorption-induced physical aging. *J. Pulp. Paper Sci*. 26:145–157.

Han, Y. J., S. Y. Yang, J. H. Park, Y. S. Chang, C. D. Eom, and H. Yeo. 2017. Separation of drying strains and the calculation of drying stresses considering the viscoelasticity of red pine wood during drying. *Drying Technol*. 35(15):1858–1866.

Hirsh, A., T. Bent, and E. Erbe. 1989. Localization and characterization of intracellular liquid-liquid phase separations in deeply frozen *Populus* using electron microscopy, dynamic mechanical analysis and differential scanning calorimetry. *Thermochim. Acta* 155:163–186.

Jiang, J. L. and J. X. Lu. 2008. Dynamic viscoelasticity of wood after various drying processes. *Drying Technol*. 26(5):537–543.

Li, Z., J. L. Jiang, and J. X. Lu. 2018. Moisture-dependent orthotropic viscoelastic properties of Chinese fir wood in low temperature environment. *J. Wood. Sci*. 64(5):515–525.

Li, Z., J. L. Jiang, and J. X. Lyu. 2020a. Moisture-dependent orthotropic viscoelastic properties of Chinese fir wood during quenching in the temperature range of 20 to –120°C. *Holzforschung* 74(1):10–19.

Li, Z., J. L. Jiang, and J. X. Lyu. 2020b. The orthotropic viscoelastic properties of Chinese fir wood during the temperature ramping process. *Drying Technol*. 38(11):1411–1420.

Peng, H., J. L. Jiang, J. X. Lu, and J. Z. Cao. 2020. Orthotropic hygro-mechanical behavior of Chinese fir during cyclical relative humidity variation. *J. Wood Sci*. 66(1):19–26.

Roig, F., G. Ramanantsizehena, F. L. Razafindramisa, E. Dantras, J. Dandurand, H. Hoyet, A. Bernés, and C. Lacabanne. 2017. Dielectric and mechanical properties of various species of Madagascan woods. *Wood Sci. Technol*. 51(6):1389–1404.

Sellevold, E. J., F. Radjy, P. Hoffmeyer, and L. Bach. 1975. Low

temperature internal friction and dynamic modulus for beach wood. *Wood Fiber* 7:162–169.

Sugiyama, M., E. Obataya, and M. Norimoto. 1998. Viscoelastic properties of the matrix substance of chemically treated wood. *J Mater. Sci*. 33:3505–3510.

Sun, N. J., S. Das, and C. E. Frazier. 2007. Dynamic mechanical analysis of dry wood: Linear viscoelastic response region and effects of minor moisture changes. *Holzforschung* 61(1):28–33.

Takahashi, C., Y. Ishimaru, I. Iida, and Y. Furuta. 2004. The creep of wood destabilized by change in moisture content. Part 1: The creep behaviors of wood during and immediately after drying. *Holzforschung* 58(3):261–267.

Zhan, T. Y., J. L. Jiang, and J. X. Lu. 2015. The viscoelastic properties of Chinese fir during water-loss process under hydrothermal conditions. *Drying Technol*. 33(14):1739–1745.

Zhan, T. Y., J. L. Jiang, J. X. Lu, Y. L. Zhang, and J. M. Chang. 2018. Influence of hygrothermal condition on dynamic viscoelasticity of Chinese fir (*Cunninghamia lanceolata*). Part 2: moisture desorption. *Holzforschung* 727:579–588.

Zhan, T. Y., J. L. Jiang, J. X. Lu, Y. L. Zhang, and J. M. Chang. 2019. Temperature-humidity-time equivalence and relaxation in dynamic viscoelastic response of Chinese fir wood. *Constr. Build. Mater*. 227:116637–116645.

Zhan, T. Y., J. L. Jiang, H. Peng, and J. X. Lu. 2016. Dynamic viscoelastic properties of Chinese fir (*Cunninghamia lanceolata*) during moisture desorption processes. *Holzforschung* 70(6):547–555.

Zhao, L. Y., J. H. Jiang, and J. X. Lu. 2016. Effect of thermal expansion at low temperature on mechanical properties of Birch wood. *Cold Reg. Sci. Technol*. 126:61–65.

Zhao, L. Y., J. H. Jiang, J. X. Lu, and T. Y. Zhan. 2015. Flexural property of wood in low temperature environment. *Cold Reg. Sci. Technol*. 116:65–69.

Zhou, F., Z. Y. Fu, Y. D. Zhou, J. Y. Zhao, X. Gao, and J. H. Jiang. 2020. Moisture transfer and stress development during high-temperature drying of Chinese fir. *Drying Technol*. 38(4):545–554.